ADJUSTABLE NEURAL NETWORK CONTROLLER: APPLICATION TO A LARGE SEGMENTED REFLECTOR

José-Alberto LUZARDO
Anastassios CHASSIAKOS
California State University,Long Beach
Long Beach, CA 90840-5602

Helen RYACIOTAKI-BOUSSALIS
California State University, Los Angeles
Los Angeles, CA 90032

Abstract

A new neural network controller (NNC) whose parameters are adjusted on line is presented to control a class of multivariable linear systems. The plant to be controlled is assumed to be square (p inputs, p outputs) and almost strictly positive real (ASPR), [2]. The NNC is applied to a linear model of a large segmented space reflector and simulation results are presented. The ASPR condition is a strong condition, in general, but for the specific application of interest, i.e. control of flexible structures, the ASPR condition can be satisfied by an appropriate combination of the output variables (positions and velocities). As compared to other adaptive NNC reported in the literature, the proposed NNC is simpler and more suitable for real time applications.

1. Introduction

Adaptive neural network controllers usually exhibit high complexity that makes their real time application difficult. This is because the number of neurons required is usually high, and the algorithms to train the NN are slow. In this paper we present a neural network controller (NNC) whose parameters are adjusted on line for the problem of disturbance rejection for a large segmented space reflector model [1]. The control algorithm is simple and can be implemented in real time. Unlike other NNCs that are reported in the literature ([7],[8]), the neural network controller proposed here requires relatively few neurons and its learning algorithm is faster than backpropagation used in [6] and [3].

Stability of the closed loop system is determined using a Lyapunov function approach. If the plant is almost strictly positive real (ASPR), stability is guaranteed with rather mild conditions and certain prior knowledge of the plant to be controlled. This stability analysis, along with the description of the plant and the NNC, is given in Section 2.

The ASPR condition as defined in [2] is introduced for the adaptive control of multivariable systems. The ASPR condition is restrictive and hinders the extension of the proposed NNC to more general systems. In [2], several methods are proposed to relax the ASPR constraint. In the present study, however, the application of interest is vibration control of flexible structures. It has been shown that for these systems the ASPR condition can be satisfied by an appropriate combination of output variables (positions and velocities, [2, Chapter 7]). Simulation results for a large segmented space reflector model [1] are shown in Section 3, and conclusions are presented in Section 4.

2. Adjustable NNC

The proposed control system is shown in FIg. 1 and is based on part of the results obtained in [4]. In the following, we describe its main characteristics.

2.1. Description of the system and the NNC

Assumption 2.1. The plant is described by the transfer matrix $\boldsymbol{G}(s)$ with a minimal space state realization:

$$\begin{aligned} \dot{\boldsymbol{x}} &= \boldsymbol{A}\boldsymbol{x} + \boldsymbol{B}\boldsymbol{u}, \\ \boldsymbol{y} &= \boldsymbol{C}\boldsymbol{x}, \end{aligned} \tag{1}$$

where $\boldsymbol{x} \in \boldsymbol{R}^n$, $\boldsymbol{u} \in \boldsymbol{R}^p$ and $\boldsymbol{y} \in \boldsymbol{R}^p$. The system (1) is totally controllable and observable.

Assumption 2.2. The system (1) is assumed to be almost strictly positive real (ASPR), i.e. there exist a gain matrix $\widetilde{\boldsymbol{K}}$ and two positive definite matrices, $\boldsymbol{P}$ and $\boldsymbol{Q}$ such that the following equations are simultaneously satisfied:

$$\begin{aligned} \boldsymbol{P}(\boldsymbol{A} - \boldsymbol{B}\widetilde{\boldsymbol{K}}\boldsymbol{C}) + (\boldsymbol{A} - \boldsymbol{B}\widetilde{\boldsymbol{K}}\boldsymbol{C})^T\boldsymbol{P} &= -\boldsymbol{Q} < 0, \\ \boldsymbol{P}\boldsymbol{B} &= \boldsymbol{C}^T. \end{aligned} \tag{2}$$

Fact 2.1. There exists a $\boldsymbol{u}^*$ such that

$$\begin{aligned} \dot{\boldsymbol{x}}^* &= \boldsymbol{A}\boldsymbol{x}^* + \boldsymbol{B}\boldsymbol{u}^*, \\ \boldsymbol{y}^* &= \boldsymbol{y}_m = \boldsymbol{C}\boldsymbol{x}^*, \end{aligned} \tag{3}$$

where $\boldsymbol{x}^*$ is the space trajectory when $\boldsymbol{u}^*$ is applied to system (1) and $\boldsymbol{y}_m$ is the desired output (reference). In order to allow $\boldsymbol{u}^*$ to be the output of a realistic controller,

0-7803-3835-9/97/$10.00 (c) 1997 AACC

$\boldsymbol{y}_m$ is assumed to have two parts: a transient response that dies out as $t \to \infty$, and a steady state response that is actually the reference to be followed. This fact is self-evident given that the system is completely controllable.

Assumption 2.3. The neural network controller (NNC) in Fig. 1 is a two layer NN with one hidden layer ($\boldsymbol{u} = \boldsymbol{N}(\boldsymbol{e})$). The internal network topology is arranged to provide the following outputs (control inputs to the plant):

$$u_i = \sum_{j=1}^{p} \left(\sum_{k=1}^{\ell} c_{ijk}(t)\sigma(\omega_{ijk} e_j + \theta_{ijk}) \right), \qquad (4)$$

where u_i is the $i\text{-}th$ component of $\boldsymbol{u}$ and e_j is the $j\text{-}th$ component of $\boldsymbol{e} = \boldsymbol{y}_m - \boldsymbol{y}$, and $\sigma(z) = \frac{1}{1+e^{-z}}$. Notice that the parameters c_{ijk}'s are time varying while the parameters ω_{ijk}'s and θ_{ijk}'s are constant. For the sake of simplicity, let us denote $\sigma(\omega_{ijk} e_j + \theta_{ijk}) = \sigma_{ijk}$, then we can write u_i as

$$u_i = \boldsymbol{\Sigma}_i^T \boldsymbol{\alpha}_i,$$

where

$$\begin{aligned} \boldsymbol{\Sigma}_i &= [\sigma_{i11} \cdots \sigma_{i1\ell}\ \sigma_{i21} \cdots \sigma_{i2\ell} \cdots \sigma_{ip\ell}]^T, \\ \boldsymbol{\alpha}_i &= [c_{i11} \cdots c_{i1\ell}\ c_{i21} \cdots c_{i2\ell} \cdots c_{ip\ell}]^T. \end{aligned}$$

Using the previous definition for $\boldsymbol{\Sigma}_i$ and $\boldsymbol{\alpha}_i$, the vector $\boldsymbol{u}$ can be written as

$$\boldsymbol{u} = \begin{bmatrix} \boldsymbol{\Sigma}_1^T & \mathbf{o}_2 & \cdots & \mathbf{o}_p \\ \mathbf{o}_1 & \boldsymbol{\Sigma}_2^T & \cdots & \mathbf{o}_p \\ \vdots & \vdots & \ddots & \vdots \\ \mathbf{o}_1 & \mathbf{o}_2 & \cdots & \boldsymbol{\Sigma}_p^T \end{bmatrix} \begin{bmatrix} \boldsymbol{\alpha}_1 \\ \boldsymbol{\alpha}_2 \\ \vdots \\ \boldsymbol{\alpha}_p \end{bmatrix} = \boldsymbol{\Phi}\, \boldsymbol{\alpha}. \qquad (5)$$

The dimensions of $\boldsymbol{\Phi}$ and $\boldsymbol{\alpha}$ are $p \times \ell p^2$ and $\ell p^2 \times 1$ respectively. $\mathbf{o}_i$ $(i = 1, \ldots, p)$ is a zero row vector with the appropriate dimensions.

Note 2.1. A more general neural network topology can also be used; but, since the plant is linear and can be stabilized by a gain matrix $\widetilde{\boldsymbol{K}}$, the neural network topology given by equation (4) is suitable to approximate such controller gain, i.e. $\boldsymbol{N}(\boldsymbol{e}) \approx \widetilde{\boldsymbol{K}}\, \boldsymbol{e}$. In this case, u_i is generated by adding the output of p different NNs, each of which provides the approximation of the element $\tilde{k}_{ij} e_j$, that is:

$$\sum_{k=1}^{\ell} c_{ijk}(t)\sigma(\omega_{ijk} e_j + \theta_{ijk}) \approx \tilde{k}_{ij} e_j, \qquad (6)$$

where $\tilde{k}_{ij}$ is the corresponding entry of $\widetilde{\boldsymbol{K}}$. A more general NN topology is considered in [4] for nonlinear systems.

Note 2.2. Without loss of generality and in order to simplify the nomenclature, we have assumed a same number of neurons (ℓ) for each NN described in (6). Indeed, different number of neurons for NNs in (6) can be considered without affecting the main results given below.

Fact 2.2. There exists a NN with constant parameter vector $\bar{\boldsymbol{\alpha}}$ that approximates the matrix $\widetilde{\boldsymbol{K}}$ in a compact set $S \subset \boldsymbol{R}^p$ that includes the origin, i.e

$$\boldsymbol{\Phi}(\boldsymbol{e})\, \bar{\boldsymbol{\alpha}} = \widetilde{\boldsymbol{K}}\, \boldsymbol{e} + \boldsymbol{\epsilon}(\boldsymbol{e}); \;\; \boldsymbol{e} \in S, \qquad (7)$$

where $\boldsymbol{\epsilon}$ is a small approximation error vector function of $\boldsymbol{e}$, and the control law $\boldsymbol{u} = \boldsymbol{\Phi}(\boldsymbol{e})\, \bar{\boldsymbol{\alpha}}$ preserves the condition ASPR. Therefore, the derivative of the Lyapunov function $V = \boldsymbol{x}^T \boldsymbol{P} \boldsymbol{x}$ along the system trajectories inside the region S is negative definite when such control law is applied and $\boldsymbol{y}_m = \mathbf{o}$, presenting the origin as the only stable equilibrium point in S.

Proof (see [4] for details). Essentially, Fact 2.2 says that the NN approximation does not alter the stability properties and the orbit structure of the original system obtained when the control law $\boldsymbol{u} = -\widetilde{\boldsymbol{K}} \boldsymbol{C} \boldsymbol{x}$ ($\boldsymbol{y}_m = \mathbf{o}$) is applied. When the ideal control is applied, the closed loop dynamical system is structurally stable since it is exponentially stable in the Lyapunov sense. Therefore, any sufficiently small perturbation in the $\boldsymbol{C}^1$ topology will preserve the orbit structure. Moreover, by adjusting the parameter vector $\boldsymbol{\alpha}$, the perturbed system obtained by substituting (7) for $\boldsymbol{u}$ in (1), that is,

$$\dot{\boldsymbol{x}} = (\boldsymbol{A} - \boldsymbol{B}\widetilde{\boldsymbol{K}}\boldsymbol{C})\, \boldsymbol{x} + \boldsymbol{B}\boldsymbol{\epsilon}; \;\; \boldsymbol{e} = -\boldsymbol{C}\boldsymbol{x} \in S, \qquad (8)$$

can have the origin as the only equilibrium point with the same eigenvectors as the ideal closed loop system [5, 4]. This is possible because NNs can approximate a continuous function and its derivatives (approximation in the $\boldsymbol{C}^m$ topology) [1], and also match a function and its derivatives at isolated points. □

Fact 2.3. There exists a NN with parameter vector $\boldsymbol{\alpha}^*(t)$ function of time such that

$$\boldsymbol{u}^*(t) = \boldsymbol{\Phi}(\boldsymbol{e}(t))\, \boldsymbol{\alpha}^*(t). \qquad (9)$$

This fact is self-evident given the structure of the NN. The system of equations (9) has in general solutions for $\boldsymbol{\alpha}^*(t)$.

Note 2.3. Notice that the *ideal* neural network controller has time varying parameters, rather than constant ideal parameters, as in the classical adaptive control.

2.2. Adaptation law and stability

Given the above conditions, we propose the following adaptation law for the NNC:

$$\dot{\boldsymbol{\alpha}} = \boldsymbol{\Gamma}_1 \boldsymbol{\Phi}^T \boldsymbol{e} - \boldsymbol{\Gamma}_1 \boldsymbol{\Gamma}_2 \boldsymbol{\alpha}. \qquad (10)$$

$\boldsymbol{\Gamma}_1$ and $\boldsymbol{\Gamma}_2$ are two symmetric positive definite matrices chosen according to design criteria. The *leakage* term $\boldsymbol{\Gamma}_1 \boldsymbol{\Gamma}_2 \boldsymbol{\alpha}$ used in robust adaptive control is included because of the time dependence of the ideal parameters (Fact 2.3). The *leakage* term is a means to prevent the parameters from growing indefinitely.

[1] At least, an approximation in the C^1 topology is required.

The control law (10) will guarantee local stability and small tracking error under certain conditions as shown in the following. In order to study the stability of the proposed neural network control system, we choose the candidate Lyapunov function:

$$V = \boldsymbol{e}_x^T \boldsymbol{P} \boldsymbol{e}_x + (\boldsymbol{\alpha} - \bar{\boldsymbol{\alpha}})^T \boldsymbol{\Gamma}_1^{-1} (\boldsymbol{\alpha} - \bar{\boldsymbol{\alpha}}), \qquad (11)$$

where

$$\begin{aligned} \boldsymbol{e}_x &= \boldsymbol{x}^* - \boldsymbol{x}, \\ \boldsymbol{e} &= \boldsymbol{C}\boldsymbol{e}_x. \end{aligned}$$

The time derivative of (11) is given by

$$\dot{V} = \boldsymbol{e}_x^T \boldsymbol{P} \dot{\boldsymbol{e}}_x + \dot{\boldsymbol{e}}_x^T \boldsymbol{P} \boldsymbol{e}_x + 2(\boldsymbol{\alpha} - \bar{\boldsymbol{\alpha}})^T \boldsymbol{\Gamma}_1^{-1} \dot{\boldsymbol{\alpha}}, \qquad (12)$$

with $\dot{\boldsymbol{e}}_x$ derived from the definition of $\dot{\boldsymbol{x}}^*$ and $\dot{\boldsymbol{x}}$ (Assumption 2.1 and Fact 2.1):

$$\dot{\boldsymbol{e}}_x = \boldsymbol{A}\boldsymbol{e}_x + \boldsymbol{B}\boldsymbol{\Phi}(\boldsymbol{\alpha}^* - \boldsymbol{\alpha}) = \boldsymbol{A}\boldsymbol{e}_x + \boldsymbol{B}(\boldsymbol{u}^* - \boldsymbol{\Phi}\boldsymbol{\alpha}). \quad (13)$$

Substituting (13) into (12) gives

$$\begin{aligned} \dot{V} = \; & \boldsymbol{e}_x^T(\boldsymbol{P}\boldsymbol{A} + \boldsymbol{A}^T\boldsymbol{P})\boldsymbol{e}_x + 2(\boldsymbol{u}^*)^T \boldsymbol{B}^T \boldsymbol{P} \boldsymbol{e}_x \\ & -2\boldsymbol{\alpha}^T \boldsymbol{\Phi}^T \boldsymbol{B}^T \boldsymbol{P} \boldsymbol{e}_x + 2\boldsymbol{\alpha}^T \boldsymbol{\Phi}^T \boldsymbol{C} \boldsymbol{e}_x \\ & -2\boldsymbol{\alpha}^T \boldsymbol{\Gamma}_2 \boldsymbol{\alpha} - 2\bar{\boldsymbol{\alpha}}^T \boldsymbol{\Phi}^T \boldsymbol{C} \boldsymbol{e}_x + 2\bar{\boldsymbol{\alpha}}^T \boldsymbol{\Gamma}_2 \boldsymbol{\alpha}. \end{aligned} \qquad (14)$$

Equation (14) can be simplified by using the ASPR equations (2) (Assumption 2.2) and equation (7) (Fact 2.2). Then, in the compact subset $S \subset \boldsymbol{R}^p$, $\dot{V}$ can be written as

$$\begin{aligned} \dot{V} = \; & -\boldsymbol{e}_x^T \boldsymbol{Q} \boldsymbol{e}_x - 2\boldsymbol{e}^T \boldsymbol{\epsilon} - 2\boldsymbol{\alpha}^T \boldsymbol{\Gamma}_2 \boldsymbol{\alpha} + \\ & 2\bar{\boldsymbol{\alpha}}^T \boldsymbol{\Gamma}_2 \boldsymbol{\alpha} + 2(\boldsymbol{u}^*)^T \boldsymbol{B}^T \boldsymbol{P} \boldsymbol{e}_x \,;\; \boldsymbol{C}\boldsymbol{e}_x \in S. \end{aligned} \qquad (15)$$

In expression (15) for $\dot{V}$, $\bar{\boldsymbol{\alpha}}$ is a constant vector, $\boldsymbol{u}^*$ is a bounded signal, and the sum of the first three terms is negative definite. If either $\|\boldsymbol{e}_x\|$ or $\|\boldsymbol{\alpha}\|$ increased beyond certain point and the relation $\boldsymbol{C}\boldsymbol{e}_x \in S$ is still valid, the negative definite quadratic terms in (15) become dominant, and thus $\dot{V}$ becomes negative, guaranteeing that the signals are bounded. If, on the contrary, $\|\boldsymbol{e}_x\|$ increases beyond the region defined by $\boldsymbol{C}\boldsymbol{e}_x \in S$, the NN approximation for the gain controller $\widetilde{\boldsymbol{K}}$ is not valid any longer and stability can not be guaranteed.

There exist positive finite coefficients β_1, β_2, β_3 and β_4 such that

$$\begin{aligned} \dot{V} < \; & -\beta_1\|\boldsymbol{e}_x\|^2 - \beta_2\|(\boldsymbol{\alpha} - \bar{\boldsymbol{\alpha}})\|^2 + \beta_3\|(\boldsymbol{\alpha} - \bar{\boldsymbol{\alpha}})\| \\ & + \beta_4\|\boldsymbol{e}_x\|; \\ & \boldsymbol{C}\boldsymbol{e}_x \in S, \end{aligned} \qquad (16)$$

and since $V(\boldsymbol{e}_x, \boldsymbol{\alpha})$ is a positive definite quadratic function of $\boldsymbol{e}_x$ and $\boldsymbol{\alpha}$, it can be showed that

$$\dot{V} < -a_1 V + a_2\sqrt{V};\; \boldsymbol{C}\boldsymbol{e}_x \in S. \qquad (17)$$

From equation (17), if $V(\boldsymbol{e}_x, \boldsymbol{\alpha})$ takes any value larger than $V_1 = (\frac{a_2}{a_1})^2$, then $\dot{V}$ is negative and $\boldsymbol{e}_x$, $\boldsymbol{\alpha}$ are bounded, provided that the NN approximation is still valid. Denote S_1 and S_2 as

$$\begin{aligned} S_1 &= \{\boldsymbol{e}_x \in \boldsymbol{R}^n \,|\, \boldsymbol{C}\boldsymbol{e}_x \in S\}, \\ S_2 &= \{\boldsymbol{e}_x \in \boldsymbol{R}^n \,|\, \boldsymbol{e}_x^T \boldsymbol{P} \boldsymbol{e}_x < V_1\}; \end{aligned}$$

then, it is easy to see that sufficient conditions to ensure stability are

$$\begin{aligned} S_2 &\subset S_1, \\ \boldsymbol{e}_x(0) &\in S_1. \end{aligned} \qquad (18)$$

In the following we point out some important remarks about the adjustable NNC presented above.

Remark 2.1. The convergence of the proposed algorithm is a local one. In [7] a global stability is obtained using sliding motion control. The strategy followed in [7] can as well be used with the adaptation law (10) to achieve global convergence. However, for the sake of simplicity and knowing that every physical system is designed to operate in its *operation range*, we do not try to achieve global stability but rather make the NN approximation cover the operation range of the system.

Remark 2.2. The objective of the NN presented here, is not to approximate the dynamical system to be controlled, but rather to emulate a hypothetical controller (not needed to be known) in order to create a region of attraction in the state space. This controller depends on the output measurements; therefore, the proposed NNC is naturally expected to have less neurons than those based on an accurate approximation of the original dynamical system.

Remark 2.3. The proposed algorithm does not guarantee zero tracking error due to the presence of the leakage term. There is a trade-off between robustness and small tracking error. This trade-off is expressed in the selection of the design parameters Γ_1 and Γ_2.

Remark 2.4. Since the plant is ASPR, the system will remain asymptotically stable with any gain that is higher than some minimal value. Therefore, the control law can be augmented to:

$$\boldsymbol{u} = \boldsymbol{\Phi}\boldsymbol{\alpha}(t) + \boldsymbol{K}_1\boldsymbol{e}, \qquad (19)$$

where $\boldsymbol{K}_1$ is a positive definite matrix, and the parameters $\boldsymbol{\alpha}(t)$ are adjusted according to the adaptation law (10). The control law (19) will increase the stability region and improve the transient response.

Remark 2.5. The ASPR condition is very strong for multivariable systems. Measurement of the full state vector will allow us to create an ASPR condition as seen in the simulations below. Another option is augmenting the plant as explained in [2].

Remark 2.6. A very interesting feature of this algorithm is the absence of reference model. The reference to follow is presented as an independent time varying signal.

3. Simulation results

In this Section, we present simulation results from applying the developed NNC to the vibration control of a segmented space reflector. The segmented space reflector shown in Fig. 2 is a typical large structure that requires the development of control laws to accomplish vibration supression, pointing and reflector shape control. The modelling of this structure has been developed in [1] as part of a NASA project that includes the construction of the reflector to be used as a testbed for the development and testing of different control technologies, sensors, actuators, and implementation of different control algorithms. In Fig.2, the primary reflector is segmented into six panels each measuring 1m in diameter. They are mounted on a lightweight supporting truss structure to form a parabolic surface. The orientation and position of each panel are controlled by three linear actuators. A set of sensors provide measurements of panel displacement. Accelerometers are mounted on each panel at the conection points of the actuators to provide additional measurements for vibration control. Disturbances acting on the primary support structure through the support bipods will degrade the image quality. The objective is to attenuate the effects of these disturbances.

A model of the plant is obtained through finite element modeling, as descibed in [1]. For preliminary control design purposes, a simplified linear model of the plant is used as in [1]. This simplified model is described by a multivariable second order equation:

$$\boldsymbol{M}\ddot{\boldsymbol{x}} + \boldsymbol{D}\dot{\boldsymbol{x}} + \boldsymbol{K}\boldsymbol{x} = \boldsymbol{B}_1\boldsymbol{u} + \boldsymbol{B}_2\boldsymbol{f}, \qquad (20)$$

where
$\boldsymbol{K}$= Positive definite symmetric stiffness matrix,
$\boldsymbol{M}$= Positive definite symmetric mass matrix,
$\boldsymbol{D}$= Damping matrix,
$\boldsymbol{B}_1$= Control influence matrix,
$\boldsymbol{B}_2$= Disturbance influence matrix,
$\boldsymbol{u}$= Control input vector,
$\boldsymbol{f}$= Disturbance force vector, and
$\boldsymbol{x}$= Vector of physical coordinates (positions).

The system (20) is in general a coupled system where the control inputs can affect in different ways any particular component of the vector $\boldsymbol{x}$.

In order to apply the NNC developed in the previous section, we need to guarantee the ASPR condition. In this sense, we follow the work of D.S. Bayard presented as a case study in [2, Chapter 7]. The case study presented in this reference includes the application of direct adaptive methods for the control of a large flexible structure. In that application the output signal $\boldsymbol{y} \in \boldsymbol{R}^p$ is a combination of position and velocity measurements

$$\boldsymbol{y} = \boldsymbol{C}(\lambda\boldsymbol{x} + \dot{\boldsymbol{x}}). \qquad (21)$$

The quantity λ is a factor which scales the position measurements with respect to rate measurements. In [2, Chapter 7] it is shown that if $\lambda > 0$ satisfies an upper bound, and if the actuators and sensors are *colocated*, i.e. matrix $\boldsymbol{C}$ is such that $\boldsymbol{B} = \boldsymbol{C}^T$, then the flexible structure satisfies the ASPR condition.

The simulations were performed for a *three-pannel subsystem* on a simplified model of the large six-panel segmented space reflector described in [1]. There are three positions to control for each panel, which gives a total or 9 positions to be controlled for the three-panel subsystem.

For the simulations, the following design parameters were chosen: $\lambda = 10^{-4}$; $\boldsymbol{K}_1 = 50$; $\boldsymbol{\Gamma}_1 = 2000\boldsymbol{I}$; $\boldsymbol{\Gamma}_2 = 0.05\boldsymbol{I}$. The quantity $-\frac{\theta_i}{\omega_i}$ represents the centers of the sigmoidal nonlinearities for each neuron. The centers of the sigmoids were chosen to cover uniformly an approximate operation range that spans the interval from -1mm to 1mm for each position. In equation (6), $\ell = 6$.

The simplified model of the segmented reflector accounts for disturbances acting on the structure through the support bipods. Three sinusoidal disturbances with frequencies close to the fundamental frequency of the structure were chosen, and the disturbance rejection capabilities of the neural controller were evaluated through simulations. The results of the simulations corresponding to panel 3 of the three-panel subsystem are shown in figures 3 through 5. These results are representative of the dynamical behavior of the whole structure. Figure 3 shows the position vector $\boldsymbol{x}$ for panel 3. A comparison of the open loop responses (dashed lines) to closed loop responses using the NNC (solid lines) shows an attenuation factor of more than 10 (20 db). Fig. 4 shows typical control inputs for panel 3, and Fig. 5 shows the variation of a typical adjustable parameter (weight) of the NNC.

4. Conclusions

A simple adjustable NNC has been presented to control ASPR systems, in particular a large segmented space reflector. The neural network controller adjusts its weights on-line and requires measurements of the positions and velocities, and that the actuators and sensors be colocated. Under these conditions the ASPR condition can be satisfied, allowing the NNC to be implemented. The NNC is simple because it adjusts the coefficients of the linear layer (output layer) of the NN. The internal parameters of the sigmoids (hidden layer) are fixed according to the operation range of the system. Special consideration is taken to uniformly distribute the centers of the sigmoids ($-\frac{\theta_i}{\omega_i}$) all over the range of operation. The simulations performed show satisfactory transient responses and a fast adaptation, although the neural weights were all initialized to zero. The disturbances are attenuated by a factor of 10 or more, and as predicted by theory, all the signals remain bounded and all position errors remain small, in the presence of external disturbances.
Acknowledgment. *The research described in this paper was supported by the National Aeronautics and Space Administration under grant #NAGW-4103.*

References

[1] Boussalis, H., Cora, S.M., & Wei Z. "The use of decentralized control in design of a large segmented space reflector". 1995 Interim Report, TR-102, California State University, Los Angeles. May 1995.

[2] Kaufman, H., Bar-Kana, I., & Sobel, K. *Direct adaptive control algorithms*. Springer-Verlag, New York. 1994.

[3] Levin, A.U., & Narendra, K.S. "Control of nonlinear dynamical systems using neural networks - Part II: Observability, Identification and Control". *IEEE Transactions on Neural Networks*, Vol. 17, No 1, pp. 30-42, Jan 1996.

[4] Luzardo, J-A. "Neural Networks for approximation and control of continuous nonlinear systems". Ph.D. dissertation, Dept. of Mathematics, The Claremont Graduate School, Claremont, CA. Jan., 1997.

[5] Luzardo, J-A, Chassiakos, A., & Rumbos, A. "Representation of first order dynamical systems using neural networks". *Proc. IEEE International Conference on Neural Networks ICNN'95*, Vol.1, pp. 496-501, Perth, Australia, 1995.

[6] Narendra, K.S., & Parthasarathy, K. "Identification and control of dynamical systems using Neural Networks", *IEEE Transactions on Neural Networks*, Vol. 1, No 1, pp. 4-27, Mar 1990.

[7] Sanner, R.M., & Slotine, J-J. "Gaussian networks for direct adaptive control". *IEEE Transactions on Neural Networks*, Vol. 3, No 6, pp. 837-863, Nov 1992.

[8] Sanner, R.M., & Slotine, J-J. "Stable adaptive control of robot manipulators using neural networks". *Neural Computation*, Vol. 7, pp.753-790, 1995.

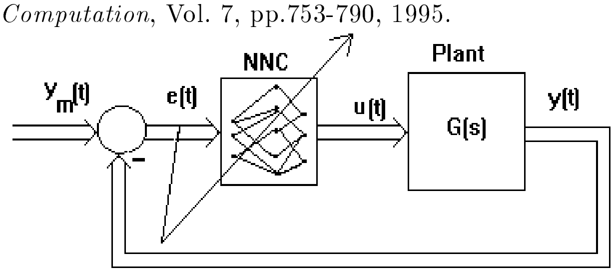

Figure 1: Adaptive NNC for linear systems.

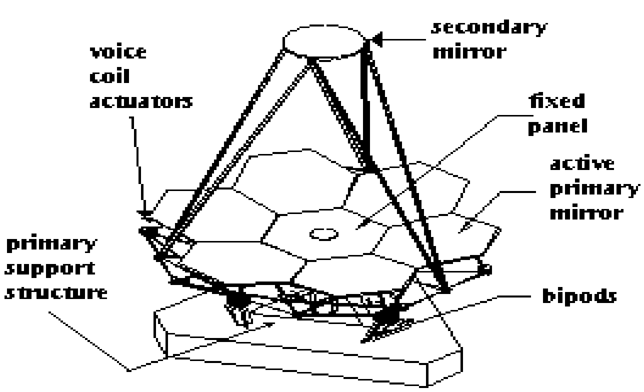

Figure 2: Segmented Reflector Telescope.

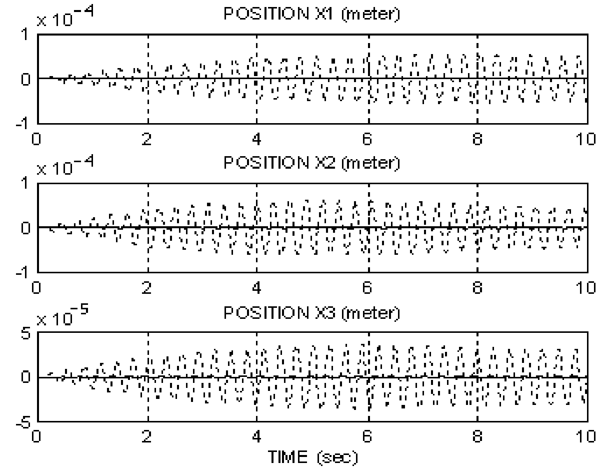

Figure 3: Positions for panel 3. Open loop (dashed) and closed loop (solid) when the adaptive NNC is applied

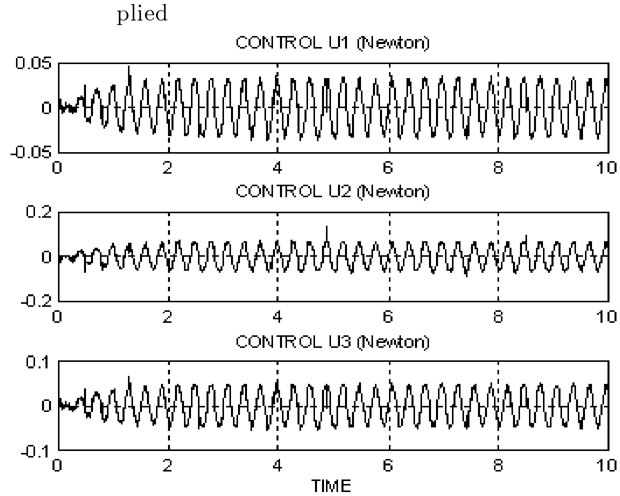

Figure 4: Control input for panel 3.

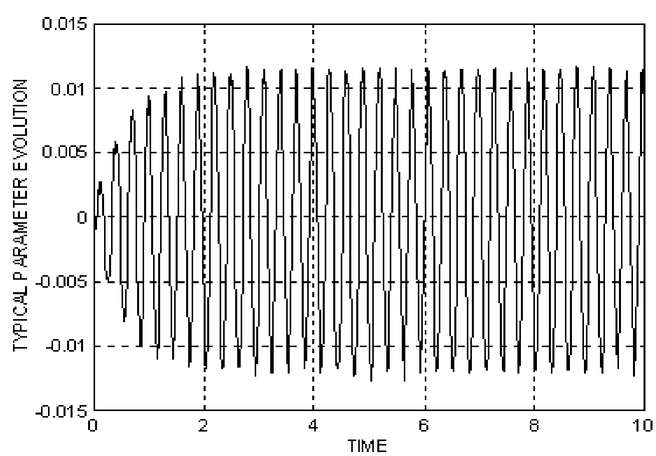

Figure 5: A characteristic behavior of the parameter estimates.